The role of ~~heat wave~~ heatwave events ~~on~~ in the occurrence and persistence of thermal stratification in the southern North Sea

Wei Chen[1], Joanna Staneva[1], Sebastian Grayek[1], Johannes Schulz-Stellenfleth[1], and Jens Greinert[2]

[1]Institute of Coastal Systems-Analysis and Modelling, Helmholtz-Zentrum Hereon, Max-Planck-Str. 1, 21502 Geesthacht, Germany

[2]GEOMAR Helmholtz Center for Ocean Research Kiel, Wischhofstr. 1-3, 24148 Kiel, Germany

Correspondence: Wei Chen (wei.chen@hereon.de)

Abstract. ~~Extremes in temperatures~~ Temperatures extremes not only directly affect the marine environment and ecosystems but also ~~have indirect impacts on~~ indirectly influence hydrodynamics and marine life. ~~The role of heat wave events responsible for~~ In this study, the role of heatwave events in the occurrence and persistence of thermal stratification was analysed by simulating the water temperature of the North Sea from 2011 to 2018 using a fully coupled hydrodynamic and wave model within the framework of the Geesthacht Coupled cOAstal model SysTem (GCOAST)~~for the North Sea~~. The model results were assessed against ~~satellite reprocessed~~ reprocessed satellite data and in situ observations from field campaigns and fixed ~~MARNET~~ Marine Environmental Monitoring Network (MARNET) stations. To quantify the degree of stratification, ~~a~~ the potential energy anomaly ~~over~~ throughout the water column was calculated. ~~A linear correlation existed between the~~ The air temperatures and ~~the potential energy anomaly~~ potential energy anomalies in the North Sea (excluding the Norwegian Trench and the area south of 54°N~~latitude. Contrary to the northern part of the~~) were linearly correlated. Different from the northern North Sea, where the water column is stratified in the ~~warming~~ warm season each year, the southern North Sea is seasonally stratified in years when a heatwave occurs. The influences of heatwaves on the occurrence of summer stratifications in the southern North Sea are mainly in the form of two aspects, i.e., a rapid rise in sea surface temperature at the early stage of the heatwave period and a ~~relatively~~ higher water temperature during summer than the multiyear mean. Another factor that enhances the thermal stratification in summer is the memory of the water column to cold spells earlier in the year. Differences between the seasonally stratified northern North Sea and the heatwave-induced stratified southern North Sea were ultimately attributed to changes in water depth.

1 Introduction

~~Recently, the increased number of extreme events with the~~ In recent decades, extreme temperature events have increased in frequency with global climate change~~has attracted more attention from research in~~ , and these events have attracted growing attention from both regional and global ~~earth systems (IPCC, 2012; Herring et al., 2015)~~research on Earth systems (IPCC, 2021; Herring et . Summer heatwaves are frequently occurring extreme meteorological events ~~that frequently occur (Perkins and Alexander, 2013) . Consequently, they cause~~ (Perkins and Alexander, 2013) that anomalously warm seawater in discrete periods via local ~~air-sea heat flux exchanges, which are also~~ air−sea heat fluxes; these periods known as marine heatwaves (MHWs) (Pearce et al.,

2011; Hobday et al., 2016). Other causes of MHWs include ocean heat transport (Rouault et al., 2007; Oliver et al., 2017) or remote forcings (Bond et al., 2015; Hu et al., 2017). ~~MHWs have been identified with a trend of increasing intensification (Oliver et al., 2020). Over~~ An increasing intensification trend of MHWs has recently been identified (Oliver et al., 2020). In this context,over the last two decades, numerous record-breaking MHW events have been reported in the Mediterranean Sea (Bensoussan et al., 2010), the Tasman Sea (Oliver et al., 2017; Perkins-Kirkpatrick et al., 2019), west Australia (Feng et al., 2013), ~~northeast~~ the Northeast Pacific (Hu et al., 2017), the western South Atlantic (Manta et al., 2018) and the East China Sea (Tan and Cai, 2018). ~~The study of MHWs has emerged as a rapidly growing field of research due to its substantial influence~~ Accordingly, due to the substantial influences of MHW events on marine hydrodynamics and ecosystems~~(Wernberg et al., 2013, 2016; Oliver et al., 2020). In the North Sea, waters are predicted to be warming fastest relative to global levels and are highly impacted by the extreme meteorological events (Smale et al., 2019; Hobday and Pecl, 2014); the concequences of MHWs however, have received much less attention (Wakelin et al., 2021)~~, the field of research on MHWs has rapidly grown (Wernberg et al., 2013, 2016; Oliver et al., 2020).

The North Sea, ~~which is~~ located on the ~~northwest European~~ passive continental margin ~~, connects to~~ of Northwest Europe, connects the Baltic Sea in the east ~~and~~ to the Atlantic through the Norwegian Sea in the north and the English Channel in the west (Figure 1). The water ~~depth is shallow in the large~~ depths in most of area of the North Sea are shallow, except for the Norwegian channel, which has an average depth of 400 m ~~deep~~ with a maximum depth of 750 m in the Skagerrak (Otto et al., 1990). The tidal circulation is dominated by the semidiurnal ~~tides~~ (M_2 and S_2) tides and interacts with the North Sea bathymetry. ~~Sources~~ Due to these relatively shallow water depths, the sources of turbulent mixing are ~~the~~ tidal currents at the bottom (Simpson et al., 1994) and ~~the~~ wind-induced waves at the water surface (Staneva et al., 2017)~~, due to the relatively shallow water depth~~. The North Sea, which is strongly impacted by extreme meteorological events, has been predicted to be warming twice faster than the global levels (Smale et al., 2019; Hobday and Pecl, 2014); nevertheless, the consequences of MHWs, have received little attention (Wakelin et al., 2021).

During the summer of 2018, extreme ~~climates~~ heatwave events with record-breaking temperatures were observed in many countries. The German Weather Service (Deutscher Wetterdienst, DWD) observed weekly temperature anomalies of up to ~~$+3 \sim 6°$~~$+3 - 6°$C (Imbery et al., 2018). In addition to ~~the~~ West and North Europe, which suffered significant social and environmental impacts~~across West and North Europe, the summer heatwave imposed large perturbations on natural processes in the North Sea~~, the North Sea (specifically, the natural processes therein) was heavily perturbed by these summer heatwaves. For example, Borges et al. (2019) found that the dissolved methane concentration in surface waters along the ~~Belgium~~ Belgian coast was three times higher during the summer of 2018 than during a normal year. ~~The European 2018 heatwave events~~ Hence, the heatwave events that struck Europe in 2018 provide a good opportunity ~~for investigating the impact of extreme climate~~ to investigate the impacts of extreme meteorological conditions on the development of density stratification in the southern North Sea. ~~An identification of~~ In particular, extreme temperature events ~~and how these may have impacts on key fish and shellfish stocks was documented~~ were identified in the recently published Ocean State Report 5, which also documented how these events may impact key fish and shellfish stocks (Wakelin et al., 2021). However, to the best of our knowledge no systematic

studies have yet investigation has been performed to explain this impact these impacts in relation to the changes in vertical stratification during extreme temperature events in the North Sea.

As a fundamental physical processIn the North Sea, the development of vertical thermal stratificationin the North Sea , a fundamental physical process, is associated with the seasonal cycling of water temperatures, especially in on the shallow shelfseas. From early May to late September, the majority of the North Sea becomes stratified, which is also known as the summer stratification (Pingree and Griffiths, 1978). Understanding the occurrence of this summer stratification and its temporal and spatial variations is important and the interest thus has been the focus of many studies (Becker, 1981; Elliott and Clarke, 1991; Pohlmann, 1996; Schrum et al., 2003; Stips et al., 2004; Sharples et al., 2006; van Leeuwen et al., 2015). In shallow shelfseasOn the shallow shelf, stratification plays an essential role in, e.g., water circulation (van Haren, 2000; Luyten et al., 2003), sediment flocculation and transport (Fettweis et al., 2014), phytoplankton growth (Nielsen et al., 1993; Fernand et al., 2013) and fishery resources (Sas et al., 2019)management (Sas et al., 2019).

Many relevant modelling studies have been conducted within the North Sea (Luyten et al., 2003; Stips et al., 2004; Sharples et al., 2006; Mathis et al., 2015). More recently , the development of Klonaris et al. (2021) recently developed a state-of-the-art three dimensional hydrodynamic model based on ROMS was demonstrated by Klonaris et al. (2021) , who showed accurately reproduced the Regional Ocean Modeling System (ROMS) and accurately reproduced the thermohaline variations in the southern North Sea. Considering the interface between the airand the ocean , models that couple Other models have been employed to investigate thermodynamic air−ocean interface processes by coupling the interactions between the air-sea system were integrated to investigate thermodynamic air-ocean interface processes (Ho-Hagemann et al., 2017; Stathopoulos et al., 2020). Staneva et al. (2021) air− and sea system (Ho-Hagemann et al., 2017; Stathopoulos et al., 2020). For instance, Staneva et al. (2021) presented a new high-resolution model (part of the Geesthacht COAstal model SysTemCoupled cOAstal model SysTem, GCOAST) that couples ocean and wave model systems for the North Sea and the Baltic Sea. This model implemented ; this model implements parameterisations that take into account the nonlinear feedback between tidal currents and wind waves. Within this framework, Chen et al. (2021) developed a three-dimensional variational (3DVAR) data assimilation scheme , which improved that improved the modelling of sea surface temperature modelling in the North Sea. In that study; then, the authors further quantified the impact of temperature assimilation on the heat budget estimates for the North Sea.

Based on a 51-year 51 years of simulation data, van Leeuwen et al. (2015) identified five regimes in the North Sea regarding different types of density stratification. The study They classified the presence of stratification according to the influence of freshwater from estuaries, permanent haline stratification in the deep Norwegian Trench, seasonal changes in air temperatures, and strong turbulent mixing by tidal currents and waves. However, these classifications fail to categorise their categories failed to categorise include approximately 30% of the North Sea area, especially in the its southern part, where the water depth is generally less than 50 m and the regime absence of a dominant stratification type accounts for approximately half of the total area . In this area, the density stratification is highly sensitive to the climate conditions and shows lacks a dominant stratification regime. The density stratification in this area is particularly sensitive to changes in climate and exhibits interannual variations. The Therefore, the present study focuses on this unclassified area , in order to quantify the role of heatwaves on in

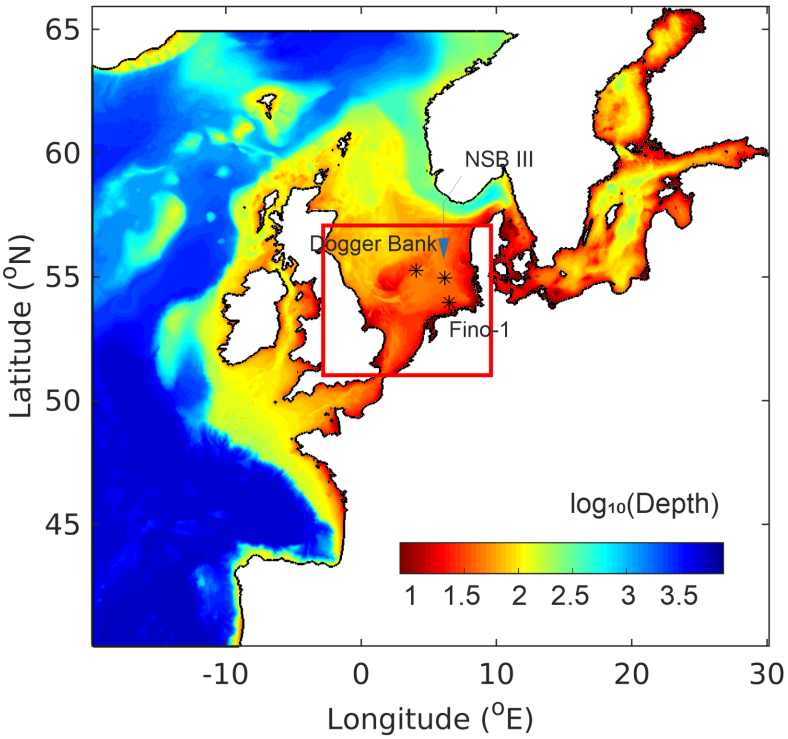

Figure 1. ~~The~~ GCOAST model domain. The bathymetry (~~meters~~m) is shown on a ~~log~~ logarithmic scale. The ~~location~~ locations of the observations from the Poseidon cruise (Dogger Bank) and MARNET stations (NSB III and Fino-1) are indicated with asterisks. The red frame defines the area of the middle and southern North Sea.

the occurrence of summer stratification. We further ~~address the question "What are the~~ seek to identify the main factors that affect the intensity and duration of the thermal stratification in the southern North Sea~~?"~~.

This study applied a fully coupled ~~hydrodynamics~~ hydrodynamic and wind-wave model ~~in~~ to the North Sea and ~~adjacent seas~~the adjacent sea areas. The model ~~simulations~~ simulation results were compared with ~~recent field measurements of~~ both short-term (a cruise campaign from 23 July to 1 August 2018) and multiyear (6-year stationary measurements) acquired in recent years. Furthermore, ~~a 38-year~~ 38 years of sea surface temperature (SST) data were reprocessed from satellite observations ~~was used~~ to detect the occurrence and duration of ~~the MHWs. Details~~ MHWs. The details of the observations and the methods used for analysis are described in the next section. The results are presented in Section 3~~contains the results~~, and the discussion follows in Section 4. The main conclusions are given in Section 5.

2 Materials and Methods

2.1 Model

This study conducted an 8-year (2011-2018) numerical simulation with the Nucleus for European Modelling of the Ocean (NEMO) ocean circulation model ~~NEMO~~ (Madec and the NEMO team, 2016) fully coupled to the wave model WAM (The Wamdi Group, 1988; Günther et al., 1992). ~~The model is set up under the framework of the Geesthacht Coupled cOAstal model SysTem (GCOAST)~~ This model allowed us to analyse the extreme year of 2018, which is a focus of our research, as well as several past heatwave events and cold spells. The model was established under the GCOAST framework covering the Northwest European Shelf, the North Sea, and the Baltic Sea, and it has a horizontal resolution of approximately 3.5 km ~~and a~~ with the vertical resolution of the NEMO standard $\sigma - z^*$ hybrid grid with 50 levels. The present study focuses on the southern North Sea, which is defined as the area ~~between $-3 \sim 9°$~~ within $-3 - 9°$E longitude and ~~$51 \sim 57°$~~ $51 - 57°$N latitude (~~shown by the~~ red frame in Figure 1).

For the boundary conditions, the temperature, salinity and barotropic forcing were derived from the hourly output of the Copernicus Marine Environment Monitoring Service (CMEMS) Forecast Ocean Assimilation Model (FOAM) Atlantic Margin Model version 7 (AMM7) ~~output~~ (O'Dea et al., 2012). Tidal harmonic constituents derived from the TPXOv8 model were applied at the open boundaries to force the tidal motions (Egbert and Erofeeva., 2002). The ~~ECMWF (~~data from the European Centre for Medium-Range Weather Forecasts(ECMWF) Reanalysis version 5 (ERA5) ~~data~~ were used at the water surface (Hersbach et al., 2020). The ~~data contained~~ ERA5 data included the air temperature 2 m above the water surface, which was also applied ~~for analysing~~ to analyse the relation between the variation in air temperature and the thermal stratification in the North Sea. The model adopted a baroclinic time step of 100 seconds. Turbulent eddy viscosities/diffusivities were computed with a 'k-ϵ' ~~closure scheme using~~ turbulence closure scheme with the generic length scale ~~turbulence model~~ (Umlauf and Burchard, 2003). Further details of the model ~~have been~~ are documented in Chen et al. (2021).

2.2 ~~Observational~~ Observation data

In-situ data were acquired by two different methods. From 23 July to 1 August 2018, ~~a field measurement was conducted at~~ field measurements were conducted in the Dogger Bank (Figure 1) during ~~the~~ Poseidon cruise POS526. This was part of a multidisciplinary research initiative of the GEOMAR Helmholtz Center for Ocean Research (GEOMAR, 2019). During the cruise, high-resolution temperature and salinity data were sampled by conductivity-temperature-depth CTD (Sea-Bird SBE 49 FastCAT) measurements. Long-term (interannual) data were further obtained from two fixed automatic oceanographic platforms in the North Sea: Nordseeboje III (NSB III, $54°41'$N and $6°47'$E) and FINO-1 ($54°00.892'$N and $6°35.258'$E)(see Figure 1~~for the locations). They~~). Both platforms are part of the Marine Environmental Monitoring Network ~~system~~ (MARNET), which is operated by the German Federal Maritime and Hydrographic Agency (Bundesamt für Seeschifffahrt und Hydrographie, BSH). On these MARNET platforms, water temperature and salinity at different depths are collected continuously and processed to ~~hourly intervals~~an hourly interval.

A ~~38-year time series SST over the 1982-2019 period was obtained by~~ time series of SST data spanning 38 years (1982 – 2019) was derived from the European Space Agency ~~Sea Surface Temperature~~ (ESA) SST Climate Change Initiative (~~ESA SST~~ CCI) Level 3 ~~products (1982-2016~~(1982 – 2016) (Merchant et al., 2019) and the Copernicus Climate Change Service (C3S) Level 3 product (~~2016-2019~~2016 – 2019). These ~~daily-mean~~ daily- mean datasets cover the European Northwest Shelf ~~Ocean~~ with a spatial resolution of 0.05~~degrees~~ ° by 0.05~~degrees~~°. The data were retrieved from the Copernicus Marine Service (https://resources.marine.copernicus.eu/).

2.3 Temperature analysis

Each calendar year was divided into two separate seasons, i.e., the ~~cooling~~ cold season and the ~~warming~~ warm season, according to the interannual trend of air temperatures~~in the annual variation~~. Normally, the ~~cooling~~ cold season lasts from ~~January to mid April and then from September to December~~September to mid-April of the following year, while the ~~warming season is from mid April~~ warm season endures from mid-April to August. In ~~cooling seasons, cold-spells may be present~~ the cold season, cold spells are considered to occur when there are ~~periods of~~ at least 5 consecutive days in which the temperature is lower than the threshold of the 10th percentile (Wakelin et al., 2021). In the ~~warming~~ warm season, MHW events are identified, following the criteria introduced by Hobday et al. (2016), i.e., when the water temperature exceeds the threshold of the 90th percentile within in a period of at least 5 consecutive days.

2.4 Quantification of stratification

As introduced by Simpson (1981), the potential energy anomaly ϕ, is frequently used as a suitable measure of the degree of stratification. This variable indicates the amount of mechanical energy (per m^3) required to instantaneously homogenise the water column with given density stratification. The parameter ϕ is defined as follows:

$$\phi = \frac{1}{D}\int_{-H}^{\eta} gz(\overline{\rho}-\rho)\mathrm{d}z, \tag{1}$$

~~in which~~ where

$$\overline{\rho} = \frac{1}{D}\int_{-H}^{\eta} \rho \mathrm{d}z \tag{2}$$

is the vertical mean water density and $g = 9.8\ \mathrm{m\ s^{-2}}$ is the gravitational constant of acceleration. The instantaneous total water depth is given by $D = \eta + H$, ~~with~~ where η and H ~~being~~ are the sea surface elevation and ~~the time mean~~ time-average water depth, respectively. Note that the water density ρ, which is not part of the standard NEMO model output, was calculated (at 1 atm) following Millero and Poisso (1981) (details are provided in Appendix A).

To quantify the vertical ~~structure of~~ stratification and evaluate its suitability, the gradient Richardson number, Ri, is computed:

$$Ri = \frac{N^2}{S^2}, \tag{3}$$

with the definition of the buoyancy frequency

$$N = \left(-\frac{g}{\rho} \frac{\partial \rho}{\partial z} \right)^{1/2}, \tag{4}$$

and the vertical shear

$$S = \left[\left(\frac{\partial u}{\partial z} \right)^2 + \left(\frac{\partial v}{\partial z} \right)^2 \right]^{1/2}. \tag{5}$$

Here, u and v are the horizontal velocity components ~~in~~ (m s^{-1}) obtained from the model in the same time ~~intervals~~ interval as those of the temperature and salinity data.

3 Results

The ~~model~~ simulation results were compared with the in-situ measurements obtained by ~~multiple operating systems~~ the Poseidon cruise and oceanographic platforms (Figure 2). The model was capable of capturing the main ~~features of the observation~~observed features. At MARNET station NSB III, which is located in the ~~centre of the~~ central eastern part of the southern North Sea (see Figure 1), the ~~model data~~ temporal variations in the simulated air temperature followed the seasonal cycles of the ~~temporal variations in the~~ observed air temperature from 2011 to 2018. ~~In the water, the difference between the observations and the model usually occurred during the warming period~~ The observed and simulated water temperatures usually diverged during the warm season of each year (May to September). The interannual cycle of the water temperature followed the interannual variation in the air temperature above the sea surface. However, the intensity of the water stratification showed no obvious seasonal pattern~~. Its appearance~~ ; instead, the thermal stratification was more related to air temperature changes. For example, large stratification occurred during the summers of 2014 and 2018, when the ~~surface-to-bottom~~ surface–bottom temperature difference was much larger than that during the periods before and after ~~. In 2015 and 2017, the surface-to-bottom~~ (the surface–bottom temperature difference was ~~unapparent, and fluctuations in air temperatures were small.~~ not apparent during 2015 and 2017, and the fluctuations in the air temperature were small). The differences between the modelled and measured water temperatures were in the range of $\pm$ 2°C, and the model error was smaller during the winter months than in the summer months.

Figure 3 further compares the ~~model~~ simulated data and observations at different locations ~~of~~ in the southern North Sea in July 2018. ~~At~~ In the Dogger Bank and ~~NSB III sites~~at the NSB III site, the model reproduced high temperatures within a thin

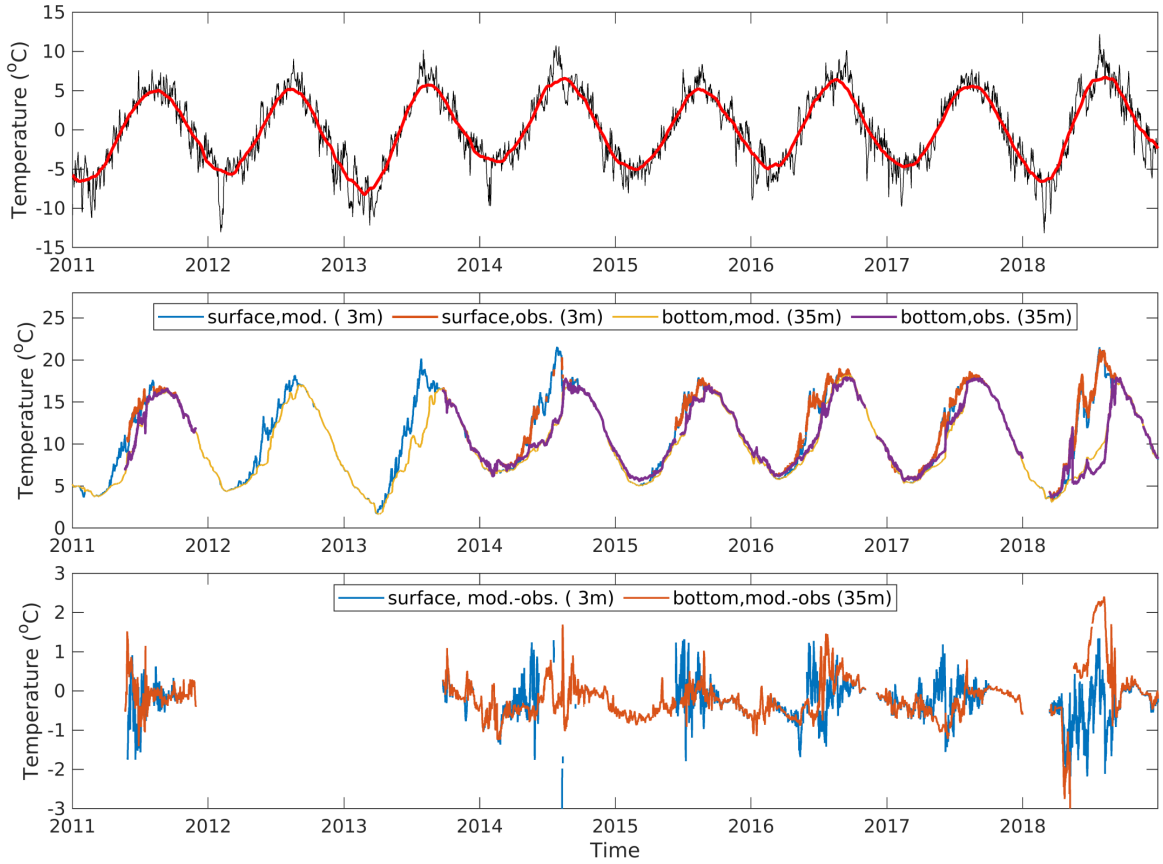

Figure 2. Upper panel: Interannual variation in the air temperature (with the multiyear mean removed) at NSB III. The black line is the daily ~~resolution~~air temperature, and the thick red line ~~is~~ represents the 3-month moving ~~averaged data~~average. Middle panel: ~~At the same location, the~~ The interannual variation in the ~~seawater temperature at the surface and the bottom from the observations~~ observed (obs.) and ~~the simulations~~ simulated (mod.) water temperatures at the surface and the bottom of the same location. Bottom panel: ~~The~~ Water temperature differences between the ~~modelled seawater temperature~~ model and the ~~observed temperature~~ in situ measurements at the surface and the bottom.

layer (approximately ~~5 ~ 10~~ 5 – 10 m) near the surface. The ~~temporal change in water temperatures mainly occurred~~ water temperature exhibited temporal variation mainly in the upper water layers (above 20 m depth). Below 20~~meters~~ m, the water temperature was relatively stable ~~, with values~~ at approximately 10°C. The differences between the surface and the bottom reached more than 15°C in both the model and the observations. At FINO-1, ~~the~~ there was almost no difference between the modelled water temperature and the in-situ measurements~~was nearly non-existent. Inconsistencies between the model and observationswere also observed~~. However, inconsistencies were observed between the simulated data and observations. The model overestimated the observations ~~at~~ in the deeper layers. ~~Below the~~ For instance, below 20~~m, e.g., at~~ m, the model yielded temperatures approximately 1 – 3°C higher than the in-situ data in the Dogger Bank and ~~NSB III, the model presented temperatures of approximately 1 ~ 3°C higher than the in-situ data~~ at site NSB III.

In general, the fully coupled model is capable of reproducing the characteristics of the water temperatures in the North Sea. The model errors were small compared to the annual water temperature variations. One reason for the discrepancies between the model and observations is that the spatial and temporal resolutions of the atmospheric forcing data are coarse. In July–August 2018, the modelled bottom water temperature was warmer than observed (Figure 2). During this heatwave period, a strong spatial temperature gradient was observed, which led to additional heat transport from shallower to deeper regions. At the NSB III site, the observed density stratification in the water column was underestimated by the model. However, considering that the model error is much smaller than the surface–bottom temperature differences (10 – 12°C), the main conclusions of the present study are unaffected.

The results were further compared with reprocessed satellite data. Figure 4 shows ~~an annual variation in~~ the annual variations in the modelled and remotely sensed SST at the NSB III platform in 2018. The ~~modelled SST was compared with the satellite reprocessed data. The~~ features of the ~~SST annual variation~~ annual SST variations at other stations were similar to those ~~of~~ at NSB III and thus are not shown. The model ~~represented~~ reproduced the satellite data from January to May and from mid-August to December ~~, with an error~~ with errors of less than 1°C. Differences between the two ~~dataset~~ datasets were mainly found from June to August, ~~where~~ when the fluctuations in the ~~satellite reanalysed~~ reprocessed satellite data were much smaller than those in the model. ~~One reason could be the smoothed measurements due to~~ This could be attributed to the smoothing of the measurements by the gridding and gap-filling of ~~level~~ Level 3 data. ~~Marine heatwave events~~ MHWs in the North Sea region were detected with the 90th-percentile threshold (Hobday et al., 2016) ~~, obtained from~~ obtained from the statistics of the 38-year time series SST ~~statistics~~data. In 2018, two MHWs were detected at NSB III: one lasting from May 24 to June 28 and another occurring from July 8 to August 5. Note that ~~May 4 ~ 15 was another period of intensive SST incline. However, it~~ the SST rose intensely during May 4 – 15; however, this period was not defined as an MHW event because of the relatively low temperatures.

Regarding the relationship between air temperature variations and the ~~occurrence of seasonal~~ seasonal cyclicity of the thermal stratification, further comparisons were made ~~between~~ among a typical normal year ~~,~~ (i.e., 2015), the extreme ~~heat wave~~ heatwave year of 2018~~and multiyear means~~ , and the multiyear mean (Figure 5). In the ~~warming period~~ warm season of 2018, there were three periods in which the air temperature was higher than the multiyear mean. The maximum air temperature anomaly reached 6°C. Correspondingly, three ~~'heat spikes' were~~ 'heat spikes' are present on the SST curve. During each

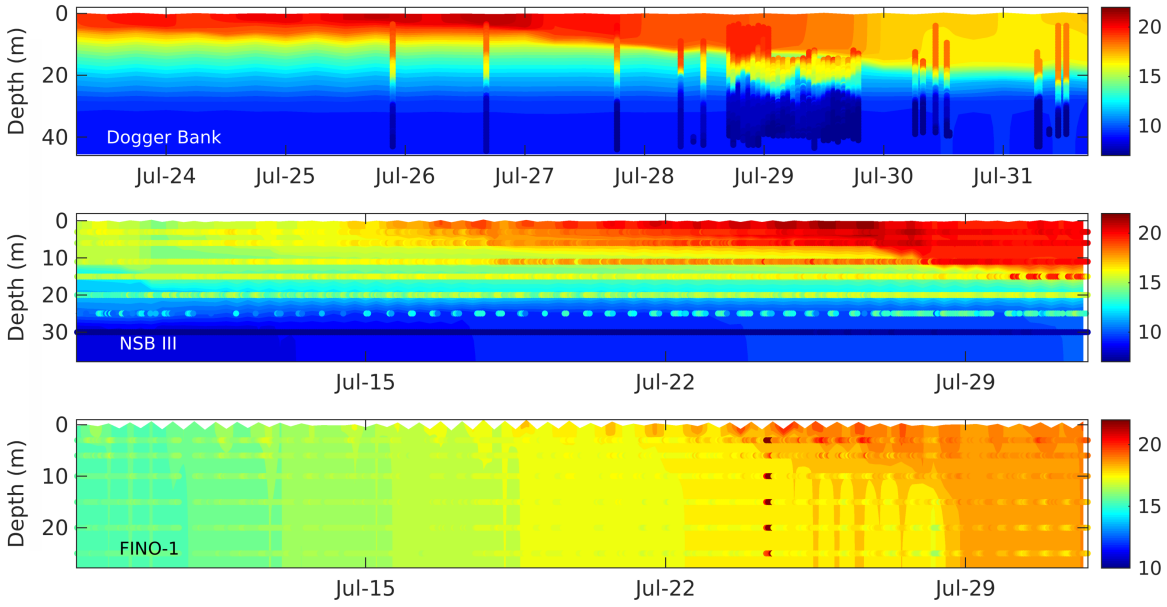

Figure 3. ~~Water~~ In situ-measured and model-simulated water temperatures (in °C) ~~of the in-situ observations and the model simulations~~ in July. In the ~~upper panel~~Dogger Bank, ~~observations are taken~~ measurements were obtained by ~~the~~ a CTD profiler during the Poseidon campaign~~and in~~ . At the ~~middle~~ MARNET stations NSB III and ~~lower panels~~FINO-1, ~~the dotted lines are MARNET data~~ temperatures were measured ~~at~~ in fixed water layers.

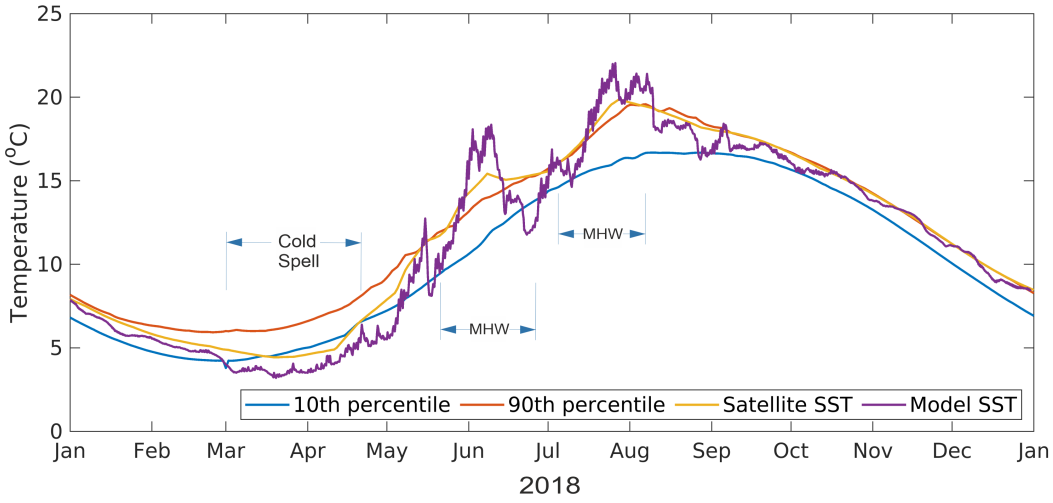

Figure 4. Annual SST variation (in °C)at the NSB III platform ~~of~~ in 2018. In addition to the satellite ~~data~~measurements (yellow curve) and the simulation results (purple curve), the ~~model simulations in 2018~~ 10th- and ~~the 10th~~/90th-percentile ~~SST of~~ SSTs from the multiyear statistics are shown. One ~~cold-spell~~ cold spell and two MHWs ~~are~~ were detected based on the 10th and 90th percentiles.

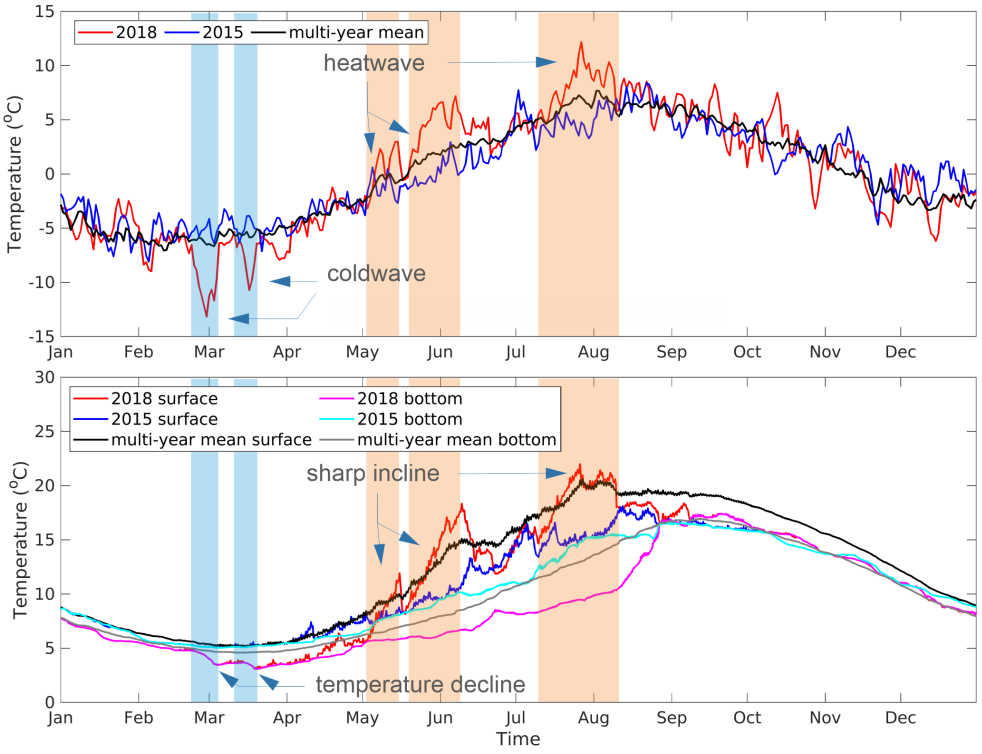

Figure 5. Upper panel: Annual variation in the simulated air temperature (with the multiyear mean removed) at NSB III for 2018 (red line), 2015 (blue line) and the multiyear mean (black line). ~~The~~ In the warm season of 2018, the periods in which the air temperature ~~increased rapidly during~~ was higher than the ~~warming season of 2018~~ multiyear mean and the SST increased are ~~demonstrated~~ delineated with orange frames. Likewise, in the early spring of 2018, the periods in which the air temperature ~~decreases rapidly in early spring~~ was lower than the multiyear mean and the SST decreased are ~~demonstrated~~ delineated with blue frames. Bottom panel: Similar to the upper panel but for the simulated ~~seawater~~ water temperature at the surface and the bottom.

~~period~~of these three periods, the SST sharply ~~inclined~~increased, whereas the water temperature in the ~~deep~~ deeper layers hardly changed. In 2015, the SST 'heat spikes' were ~~present in the SST associated with a rapid air temperature increase~~ associated with rapidly increasing air temperatures from June to July. However, ~~contrary~~ in contrast to the summer of 2018, the summer of 2015 was colder than the ~~average during the warming season~~ warm season average, with the maximum air temperature anomaly being 3°C lower than the multiyear mean.

In the absence of turbulent mixing, high air temperatures (warmer ~~summer~~summers) lead to ~~a high SST~~ high SSTs and intensify the ~~temperature differences between the local sea surfaceand the bottom . This can be seen~~ local surface–bottom temperature differences. This is evident in the three ~~'heat spike'~~ 'heat spike' periods in 2018. Note that the first 'heat spike' in 2018 ~~, the first 'heat spike'~~ was not identified ~~in~~ as an MHW event due to the relatively low ~~temperature. In 2015~~temperatures

therein. Furthermore, no atmospheric heatwave or MHW events were detected ~~.~~ in 2015. Correspondingly, the SST was below the average, and the ~~surface-to-bottom~~ surface–bottom temperature difference was smaller than the multiyear mean.

~~The~~ Seawater exhibits a longer memory of ~~seawater than that of air to low temperatures leads to~~ low temperatures than does the atmosphere; this leads to a larger and more stable ~~temperature~~ thermal stratification. As shown in Figure 5,at the end of February ~~to middle March~~ into mid-March 2018, there were two ~~periods of 'cold waves'~~ cold spells with air temperatures 7°C lower than the ~~multiple-year mean. As a~~ multiyear mean. In response, the seawater was colder than usual, causing the bottom temperature to be 2°C lower than the average. This low-temperature signal remained much longer in the water than in the atmosphere and yielded colder bottom ~~water~~ temperatures over the entire ~~warming~~ warm season.

The monthly mean spatial distribution of ~~the potential energy anomaly (ϕ)~~ in the southern North Sea in 2018 (Figure 6) provides an overview of the seasonal cycle of ~~water~~ thermal stratification development during ~~the extreme temperature conditions~~extreme temperature events. The water ~~become stratified~~ column was considered to be stratified when ϕ exceeds 50 J m^{-}3, which implies the amount of energy required to instantaneously homogenise a 60 m deep water column with a surface–bottom density difference of 1 kg m^{-3}, where 60 m is approximately the average water depth of the North Sea (excluding the Norwegian Channel). The water becomes stratified by April in the northern part of the domain, i.e., ~~the north side~~ to the north of the 50~~m isobath. From May to August, the stratification developed~~ m isobath, whereas to the south, density stratification hardly occurs in the winter months (December through February), except off the Dutch coast and the German Bight. The potential energy anomaly increases after April, while stratification develops in the area north ~~to~~ of 54°N latitude ~~. South of the 50 m isobath, the~~ from May to August. The potential energy anomaly ~~reached~~ reaches 400 J m^{-3} on average from July to early August, with a maximum value of approximately 800 J m^{-3} in the area between the Dogger Bank and MARNET station NSB III. In September, the 50 J m^{-3} isoline ~~retreated~~ retreats to the north of the 50 m ~~depth line. South~~ isobath. Moreover, south of 54°N latitude, the water column ~~was~~ is mostly well mixed~~. The~~ , and the stratification near the Dutch coast and the German Bight ~~was due~~ is attributable to river runoff.

~~To illustrate inter-annual~~ The intensity of the summer stratification varies over time. To illustrate the interannual variability of the water stratification in the southern North Sea, the potential energy anomaly of each year ~~to the multi-year meant~~ relative to the multiyear mean (2011-2018) is computed by averaging ~~for threemonths~~ the anomalies over a three–month period from June to August (the main ~~stratified~~ stratification period, see Figure 6). The results are shown in Figure 7. In ~~the years~~ 2013, 2014 and 2018, the stratification is stronger than the average, whereas, in the other years~~it~~ , the stratification is weaker. In the ~~area~~ areas where the water depth is ~~less~~ shallower than 50~~meters~~ m, the largest ~~inter-annual~~ interannual variation occurs between ~~3-8~~3 and 8°E longitude and north to 54°N latitude. The mean potential energy anomaly is ~~300 ~ 400~~ 300 – 400 J m^{-3} higher than the multiyear mean in 2018, while it is ~~200 ~ 300~~ 200 – 300 J m^{-3} lower than average in 2015. Note that the largest ~~inter-annual variations of~~ interannual variations in the stratification occur in the ~~east~~ eastern part of the southern North Sea.

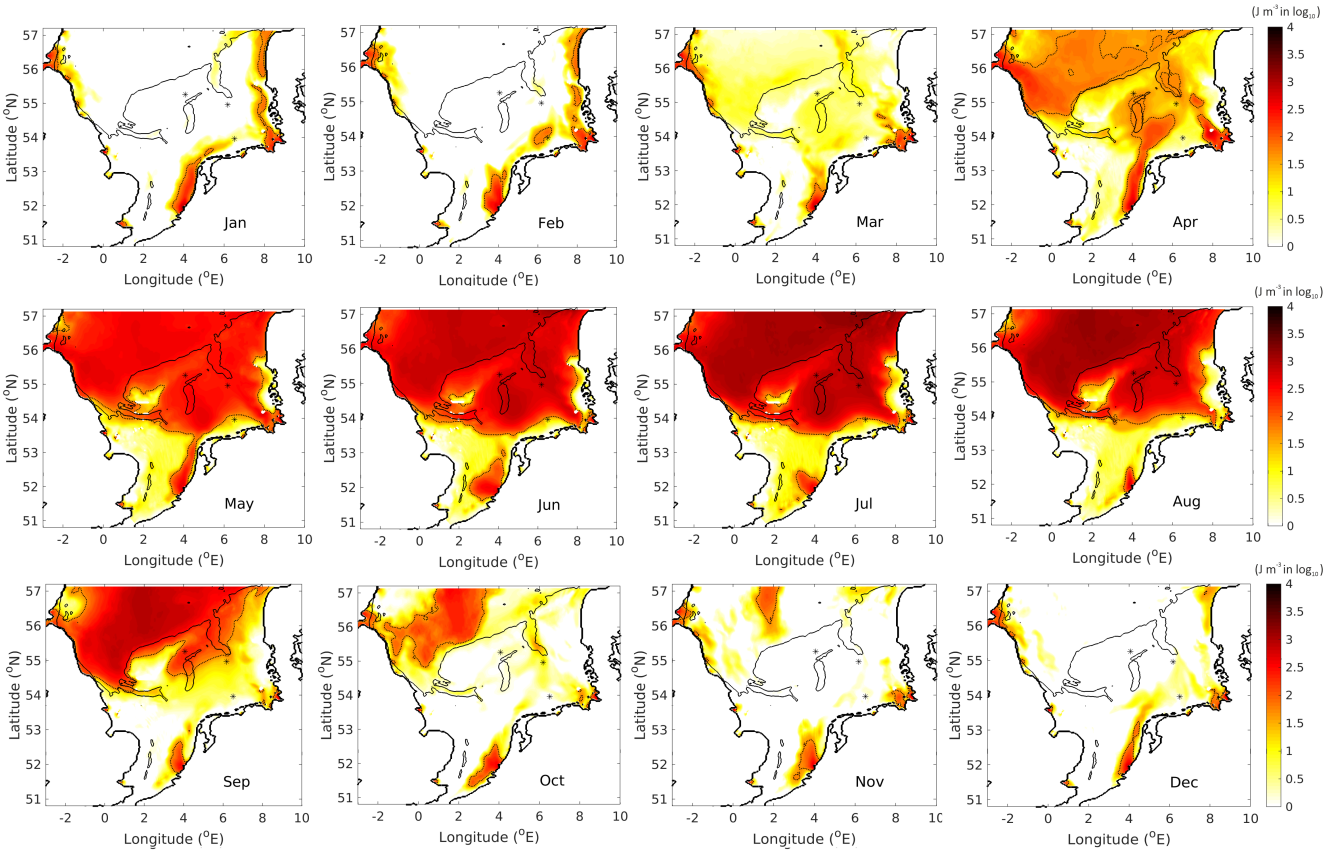

Figure 6. Evolution of the monthly mean potential energy anomaly ϕ (see ~~equation~~ Eq. 1, unit: J m^{-3} ~~in log10~~ on a $\log_{10}$ scale) ~~in~~ for 2018. ~~Dashed~~ The dashed line indicates the location where $\phi = 1.7$ J m^{-3} on $\log_{10}$ scale (or $\phi = 50$ J m^{-3}). The water column is considered to be stratified when ϕ is above this value. Thin black lines indicate the location of the 50 m ~~depth~~isobath.

4 Discussion

As illustrated in Figures 6 and 7, the stratification/destratification process in the North Sea was temporally and spatially dependent. The data analysed at a single point ~~was~~ were incapable of revealing a complete image of the relationship between the seasonal thermal stratification and the varying air temperatures in the North Sea. van Leeuwen et al. (2015) investigated the physical conditions in the North Sea ~~,~~ and attributed regimes of different types of stratification to ~~thermal-induced~~thermally induced, salt-induced, river-induced and turbulent tidal mixing. They found that in the southern North Sea, a large area could not be characterised by a dominant physical mechanism. ~~With the focus on thermal-induced stratification, we analysed~~ Focusing on thermally induced stratification, the relation between the variation in air temperature and the seasonal thermal stratification in the North Sea ~~. A~~ was analysed. The correlation coefficient R ~~that indicates a~~ reflecting the linear correlation between the air temperature and the potential energy anomaly for the summer of 2018 was computed~~and mapped, as shown~~ , and its

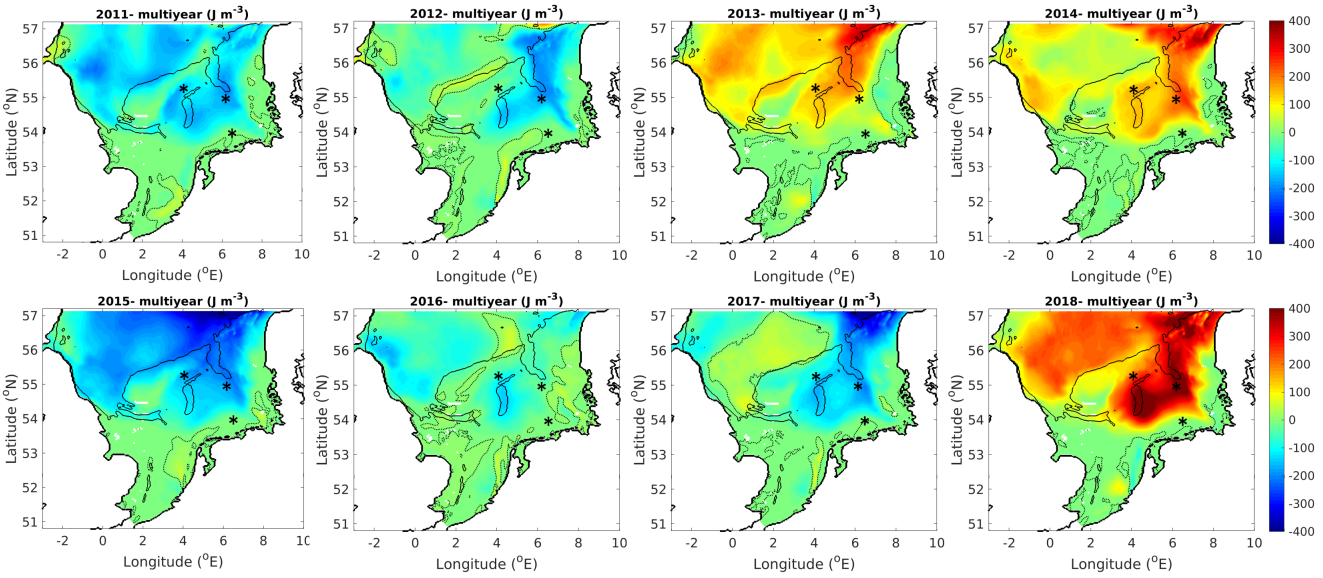

Figure 7. ~~The difference~~ Difference in the ~~three-monthly mean (June, July, August)~~ potential energy anomaly (J m^{-3}) averaged over three month (June, July and August) between a specific year and the multiyear mean. ~~Dashed~~ The dashed line indicates $\phi = 50$ J m^{-3}. Thin black lines indicate the location of the 50 m ~~depth~~isobath.

distribution is mapped in Figure 8. ~~The coefficient~~ High coefficients ($R > 0.8$~~was~~) were obtained mainly in the middle and northern parts of the North Sea (Figure 8a). This area ~~was~~ is consistent with the regime of seasonal stratification identified in van Leeuwen et al. (2015). Closer to the coast, ~~a~~ lower R ~~was~~ values were obtained. Five scattered locations in the southern North Sea were selected regarding the different values of R (see Figure 8a) ~~and scattered~~ based on the air temperature versus potential energy anomaly (Figure 8b). Note that both the Dogger Bank and the NSB III ~~are stations~~ site are located in the ~~regime~~ region for which the stratification type was unclassified in van Leeuwen et al. (2015). A linear correlation existed between the increase in air temperature and the increasing stratification, with $R = 0.8$ at ~~Northsea Mid~~ the Northsea Mid site and $R = 0.7$ at the Dogger Bank. The larger potential energy ~~anomaly~~ anomalies in the middle and northern North Sea (see 'Northsea Mid' in Figure 8a) ~~was due~~ were attributed to the deeper water ~~depth~~depths therein. At NSB III, $R = 0.5$ ~~also illustrates~~ similarly reflects a linear increase in stratification with the air temperature. ~~At~~ Off the Dutch Coast and along the Norwegian Trench, R was negative~~. For~~ ; at the former location, the water column was stratified due to river runoff, ~~and for~~ while at the latter, the water was permanently stratified. The potential energy anomaly was uncorrelated with the air temperatures at the two locations.

Mapping the correlation between the air temperature and the potential energy anomaly for different years yielded similar spatial patterns and values of R in the North Sea except for the middle part of the southern North Sea, where lower R values were found for the years with relatively ~~colder~~ cold summers. For example, in 2015, R fell by 0.1 ~~–~~ – 0.3 in the area between the Dogger Bank and NSB III (not shown), indicating a much lower correlation between the summer stratification and air temperature.

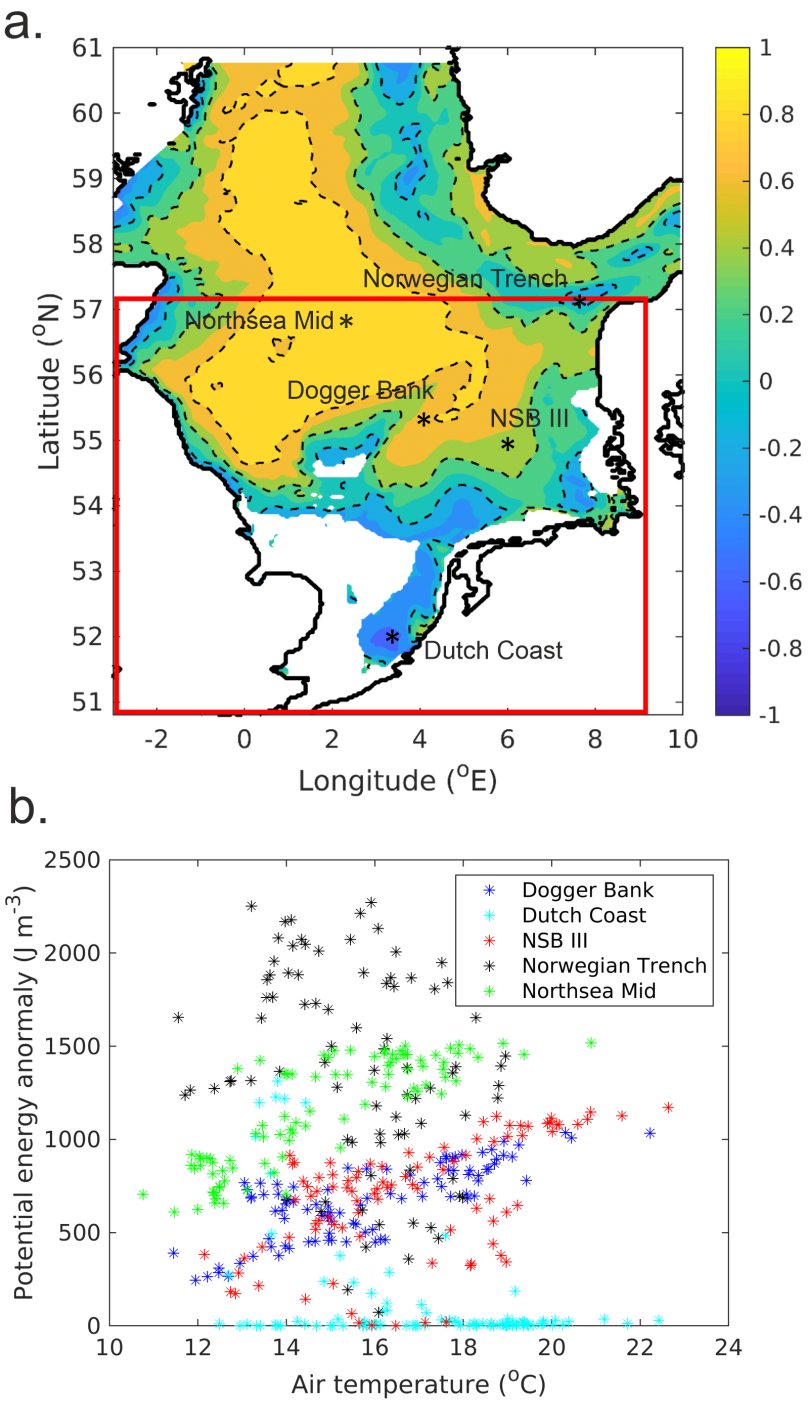

Figure 8. (a): Computed correlation coefficient ~~'R'~~ R between the air temperature and the potential energy anomaly for summer 2018 (~~June–August~~June, July and August). Note that the area with no stratification ($\phi < 50$ J m^{-3}) is ~~cut off~~excluded. Dashed contours indicate $R = 0, 0.4$ and 0.8. (b): ~~The relationship~~ Relationship between the air temperature and the potential energy anomaly in the different regimes of the North Sea. The locations are illustrated in (a). The red frame indicates the region of the southern North Sea.

Similar to ~~that of~~ Figure 4, the MHW events for each ~~warming~~ warm season (May 1 to August 31) ~~of~~ during the simulation period 2011~~–~~2018 were detected, and the number of MHW days ($\mathcal{M}$) was counted. Then, the changes in $\mathcal{M}$ with respect to its multiyear mean $\sum_{i=1}^{n} \left|\mathcal{M}_\mathrm{i} - \overline{\mathcal{M}_\mathrm{n}}\right|$ was computed for the modelling period. Here, "n $= 1,\ 2,\ 3, \ldots$" ~~counts~~ denotes the number of years~~. The~~ , and an overline $(\bar{\cdot})$ denotes the multiyear mean. Similarly, the number of days ($\mathcal{N}$) that the water column was stratified ($\phi > 50$ J m^{-3}) and the changes in stratified days $\sum_{i=1}^{n} \left|\mathcal{N}_\mathrm{i} - \overline{\mathcal{N}_\mathrm{n}}\right|$ were computed. ~~The~~ Finally, the sensitivity of stratification to the occurrence of heatwaves was quantified with the ratio ~~between the varying~~ r between the change in the number of heatwave days and ~~varying water-stratified~~ the change in the number of water stratification days:

$$r = \frac{\sum_{i=1}^{n} \left|\mathcal{N}_\mathrm{i} - \overline{\mathcal{N}_\mathrm{n}}\right|}{\sum_{i=1}^{n} \left|\mathcal{M}_\mathrm{i} - \overline{\mathcal{M}_\mathrm{n}}\right|}. \tag{6}$$

Note that the region where no MHW events were detected ($\mathcal{M} = 0$) was not considered. Figure 9 shows the spatial distribution of r in the North Sea~~. The value of~~ , where r varies between ~~0 ~ 1.~~ 0 and 1. When $r = 0$, the number of days ~~that~~ when the water column is stratified does not change interannually. This pattern occurs for both permanently stratified regions and permanently mixed regions. The former was found in the Norwegian Trench and the latter was ~~mainly found in the west~~ found mainly in the western part of the southern North Sea, as well as in the shallow shoal of the Dogger Bank, along the Danish coast and in the southern part of the German Bight. ~~If the ratio~~ In contrast, when $r = 1$, ~~i.e., the changes~~ the change in the number of water stratification days ~~equal the~~ equals the change in the number of MHW days, ~~it~~ which illustrates the dependence of the thermal stratification on the occurrence of MHWs. In the region where the water depth ~~was~~ is greater than 50~~m~~ m, $r < 0.2$. This region ~~was~~ is consistent with the region where $R > 0.6$, where stratification ~~seasonally occurs with annual varying air temperature. South to~~ occurs seasonally with annually varying air temperatures. South of the 50~~m depth~~ m isobath, $r > 0.3$ and increased towards the coasts, indicating an enhanced influence of MHWs on water stratification. The region where r ~~reached the maximum~~ peaked was between 6.5°E and the Danish coast. It is worth noting that an MHW causes density stratification within the water column, and that the resulting stratification hampers the transfer of heat along the water column and intensifies the occurrence of an MHW.

Large values ~~for~~ of r were also observed between the MHW-induced stratification region and the permanently mixed region and near the ~~UK coast~~ United Kingdom coastline in the northern North Sea. These regions are shallow and mostly mixed by tides. The water stratification is due to the short and intensive increase in air temperature. As shown in Figure 5, three periods of stratification ($\phi > 50$ J m^{-3}) were detected. Similar to ~~the counting of MHW days , we counted~~how MHW days were counted, the number of days from May to August ~~of 2011–2018~~ during 2011–2018 in which the air temperature sharply increased was obtained. In the present study, the criterion was set to 0.2°C/day, i.e., the air temperature increase rate was at least two times larger than the ~~warming period averaged increase rate of~~ rate of increase in the multiyear mean averaged over the warm season (see Figure 5, upper panel). After applying Eq. 6, ~~a~~ the ratio between the ~~changes in intensive air temperature~~ change in the number of days in which the air temperature intensively increases and the ~~changes~~ change in the number of water stratification days was obtained (see Figure 10). Overall, the spatial distribution of ~~the ratio between the changes in intensive air temperature~~

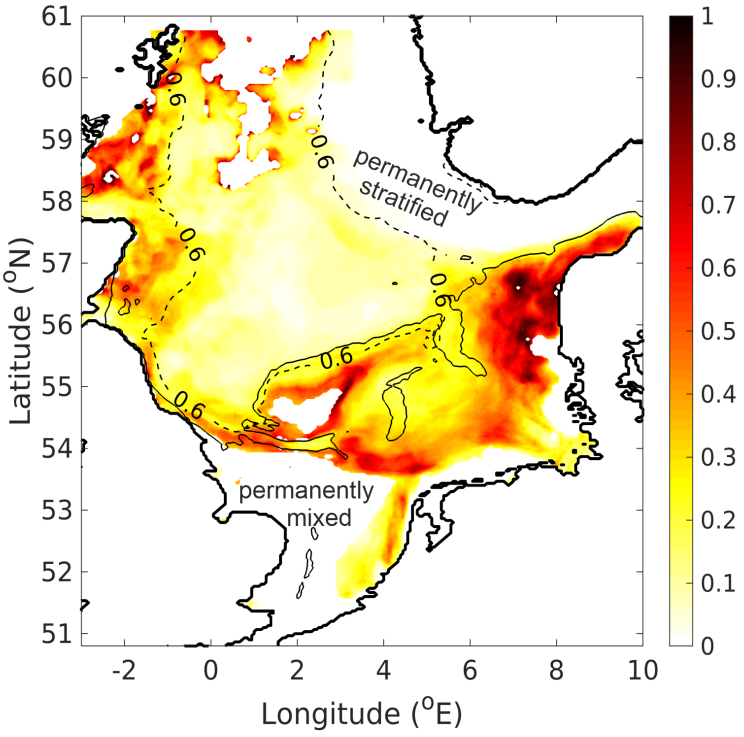

Figure 9. ~~The ratio between~~ Ratio of the number of water stratification days ~~when~~ to the ~~water was stratified and the~~ number of ~~days with~~ MHW ~~events~~days. The dashed contour line corresponds to the correlation coefficient ~~'~~$R = 0.6$ ~~'~~between the air temperature and the potential energy anomaly for the multiyear mean of the summer time~~of~~. The thin solid line indicates the ~~multiyear mean~~50 m isobath.

~~increases and the changes in water stratification~~ this ratio was similar to that of the ratio between the changes in ~~MHW days and the~~ the numbers of MHW and water stratification days. This was particularly ~~found~~ true in the area adjacent to the tidal mixing zone and the MHW-induced stratification zone~~. The region was~~ ; this region is consistent with the intermittently stratified
325 domain characterised by van Leeuwen et al. (2015). It is also important to stress the role of the winter˘spring cold spell, which reduces the SST (see Figure 4), thus increasing the vertical instability of the water column and enhancing vertical mixing. This results in the seawater being colder than average before the summer temperature rises, especially in the deeper water layers, via the redistribution of the heat through the water column. Hence, a more persistent thermal stratification is likely to be obtained in the southern North Sea.

330 The sensitivity of thermal stratification to ~~summer heatwaves~~ the occurrence of an MHW was related to changes in water depth. Figure 11 presents the annual variation in the gradient Richardson number R_i for the selected stations with different depths in the regime where $R \geq 0$ (see Figure 8). The water column was considered stably stratified when $\log_{10}(R_i) \geq 1$~~,~~; i.e., the buoyancy was an order of magnitude larger than the vertical shear. ~~For~~ In both 2015 and 2018, the water column became stratified from May to September in the middle of the North Sea, ~~with a comparable value of the gradient~~ exhibiting comparable

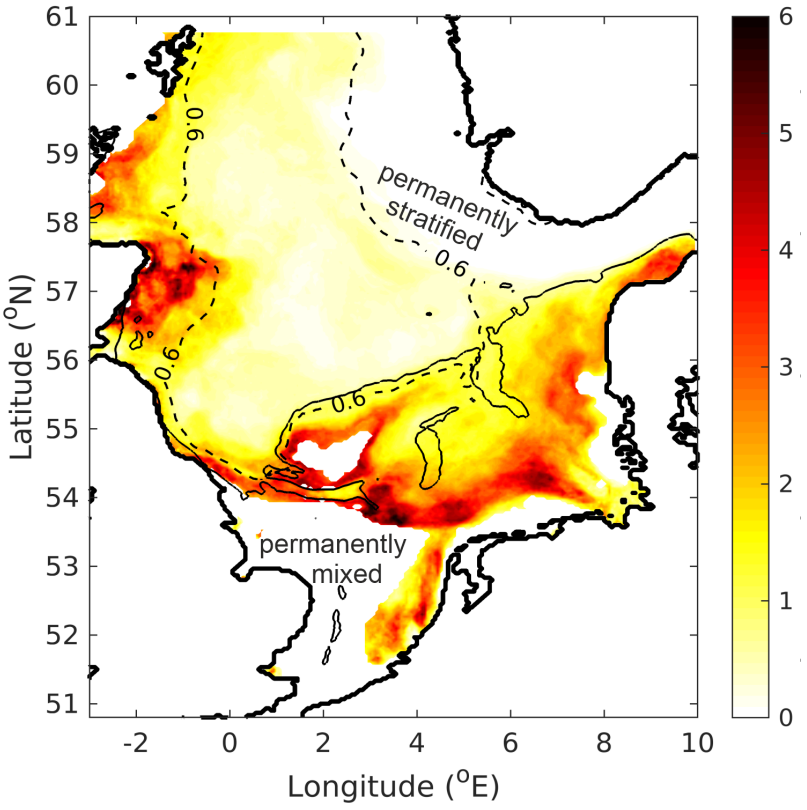

Figure 10. ~~The ratio~~ Ratio between the number of days when the water is stratified and the number of days ~~in intensive~~ when the air temperature ~~incline~~intensively increases. The contour line with a value of 0.6 indicates the area with a correlation coefficient ~~'~~$R = 0.6$~~'~~ between the air temperature and the potential energy anomaly for the ~~summer time of the~~ multiyear mean of the summertime. The thin solid line indicates the 50 m isobath.

values of R_i. ~~While approaching the coast , the gradient~~ Approaching the coast (with decreasing water depth), R_i ~~decreases with the reduced water depth~~decreases. At Fino-1, the water column was mostly well-mixed, despite some intermittent stratifications on the time scale of ~~1 ~ 2~~ 1 – 2 days. Differences between 2015 and 2018 were observed ~~at~~ in the Dogger Bank and at NSB III. ~~At~~ In the Dogger Bank, stratification occurred from June to the end of August in 2015, which was both shorter and less intensive than the same period in 2018. At NSB III, stable stratification existed only in 2018.

Further analysis of the vertical distribution of ~~the gradient~~ R_i revealed that the maximum value of R_i was obtained in the middle of the water column. At the Northsea Mid, ~~it was located~~ the peak was located at a depth of approximately 35~~m in depth~~ m. Below 45 m, $\log_{10}(R_i) \sim 0$, and the water column was homogeneous throughout the entire year. At NSB III, the period in which ~~the~~ large R_i values ~~occurred~~ were recorded was consistent with the occurrence of MHW events. In 2018, $\log_{10}(R_i) \geq 1$ during June and from early July to August. Moreover, in the Dogger Bank and at NSB III~~that~~ , the maximum R_i shifted from the upper water layers ~~down~~ to the bottom ~~with the value increased~~ during the early stage of the ~~warming~~ warm

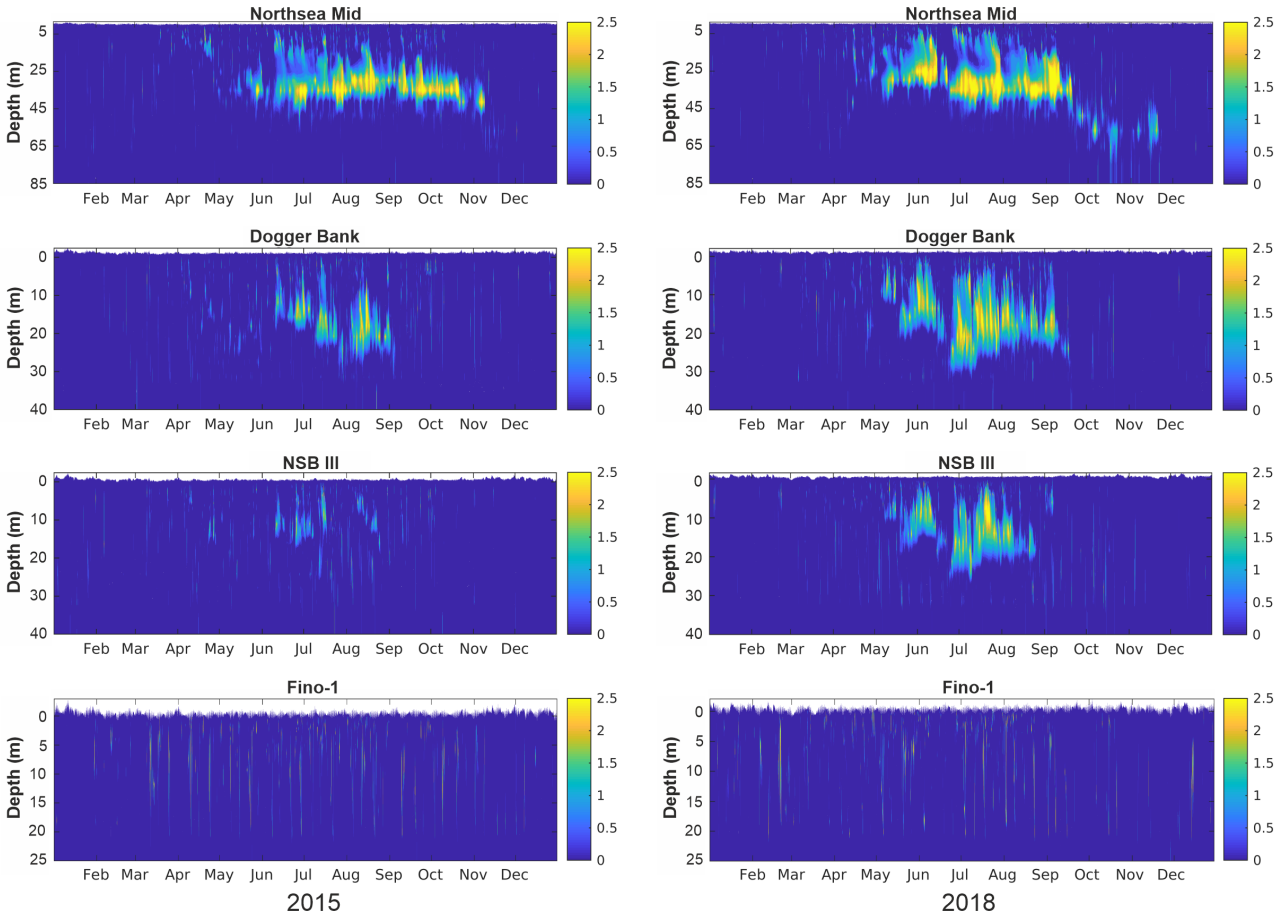

Figure 11. Gradient ~~Ri~~ Richardson numbers R_i for 2015 (left column) and 2018 (right column) at the Northsea Mid, Dogger Bank, NSB III and Fino-1 on a ~~log10~~ $\log_{10}$ scale.

season. However, in the late ~~warming~~ warm season (July and August), the maximum R_i remained in the middle water layers. At both Dogger Bank and NSB III, the water column below ~~the~~ 25~~m depth~~ m was homogeneous throughout the entire year. At Fino-1, the water depth (25 m) was too shallow to maintain long-term stable stratification.

Note that the present study takes into account the impact of ocean waves on circulation. Such an impact usually results from different processes, e.g., turbulence due to breaking/nonbreaking waves and the transfer of momentum from breaking waves to currents (Davies et al., 2000; Babanin, 2006; Breivik et al., 2015). The latter is important in shallow waters such as the Baltic Sea (Alari et al., 2016) and the North Sea (Staneva et al., 2017; Wu et al., 2019). By including wave-induced turbulent mixing, the simulation was capable of resolving the turbulent mixing length and modelling the vertical stratification and circulation in the North Sea (Staneva et al., 2017, 2021), especially near the coastal zones. Figure 12 shows the modelled seasonal mean mixed layer depth (MLD) of the coupled NEMO-WAM model run in 2018 and the relative changes when comparing the fully coupled run with the uncoupled run, i.e., $(\mathrm{MLD}_{\mathrm{coupled}} - \mathrm{MLD}_{\mathrm{uncoupled}})/\mathrm{MLD}_{\mathrm{coupled}} \times 100\%$. Following the annual water

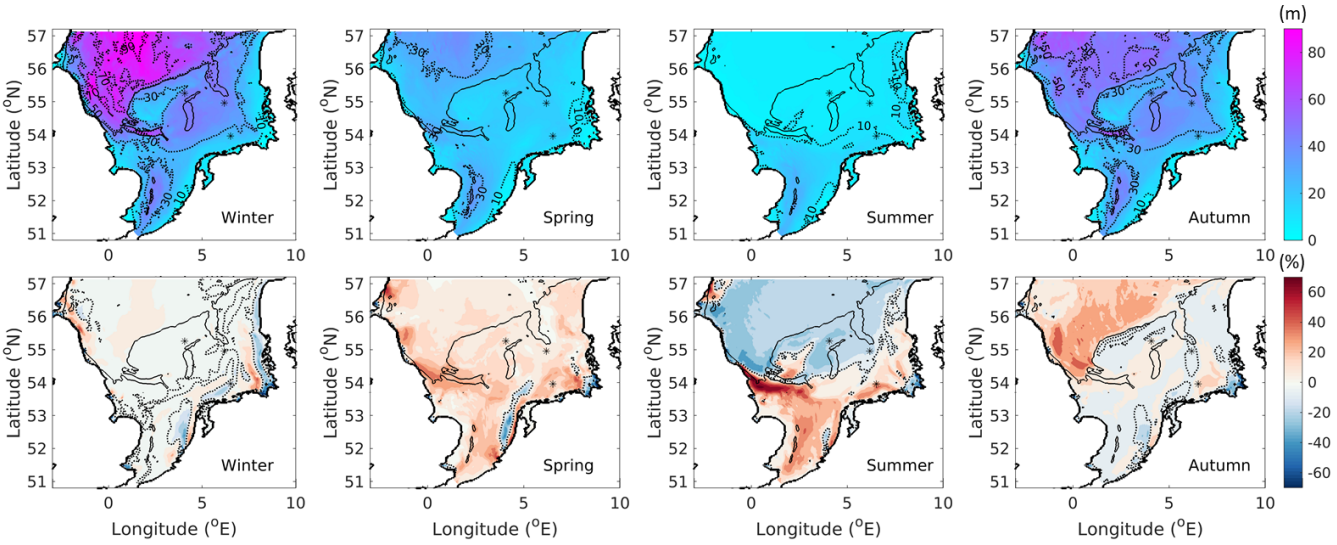

Figure 12. Upper panels: The seasonal mean mixed layer depth (MLD) of the coupled NEMO-WAM model run. Lower panels: The relative changes in the MLD when comparing the coupled run with the stand-alone NEMO (uncoupled) run. Dotted lines in the lower panels indicate the 0% contour.

temperature cycle, the MLD in the southern North Sea decreases from winter to summer and rises again in autumn. The MLD changes more quickly in deeper regions than in shallow coastal areas. There is almost no seasonal cycle along the coast of the German Bight. The large difference in the MLD between the coupled and uncoupled runs is found from spring to autumn, when stratification develops with the changing air temperature. In summer, the MLD of the coupled run is approximately $20-40\%$ larger than that of the uncoupled run in the southern North Sea, whereas it is approximately 20% smaller north to the $54°$N. In autumn, the stratification disappears in the southern North Sea, where the MLD differences drop between -10 and 10%. In the north, where the water depth is deeper than 50 m, the MLD of the coupled run is approximately 20% larger than the MLD of the uncoupled run.

Wave-induced processes also change the heat fluxes at the water surface (Figure 13). The net heat flux is positive overall (from the air to the sea) in spring and summer and negative (from the sea to the air) in winter and autumn. The importance of wave forcing for ocean predictions in the North Sea has been demonstrated by Staneva et al. (2017). Wave-induced processes impact the distribution of the heat fluxes. In summer, in the southern North Sea, the fluxes increase by approximately $20-40\%$, while a reduction of $20-50\%$ occurs along the coastal, well-mixed area of the German Bight. For further details of ~~the wave impact~~these wave impacts, refer to the Supplemental ~~materials for~~ Materials for the results of the model ~~that~~ run where NEMO was uncoupled with WAM.

Apart from circulation-wave coupling, the stratification itself also ~~influenced circulation. On a time mean momentum budget, where baroclinic forcing balances the internal friction, turbulent eddy viscosity decreases while turbulence is eliminated by the increasing degree of stratification. Baroclinic circulation is~~ influences the circulation. Baroclinic circulation, a result of

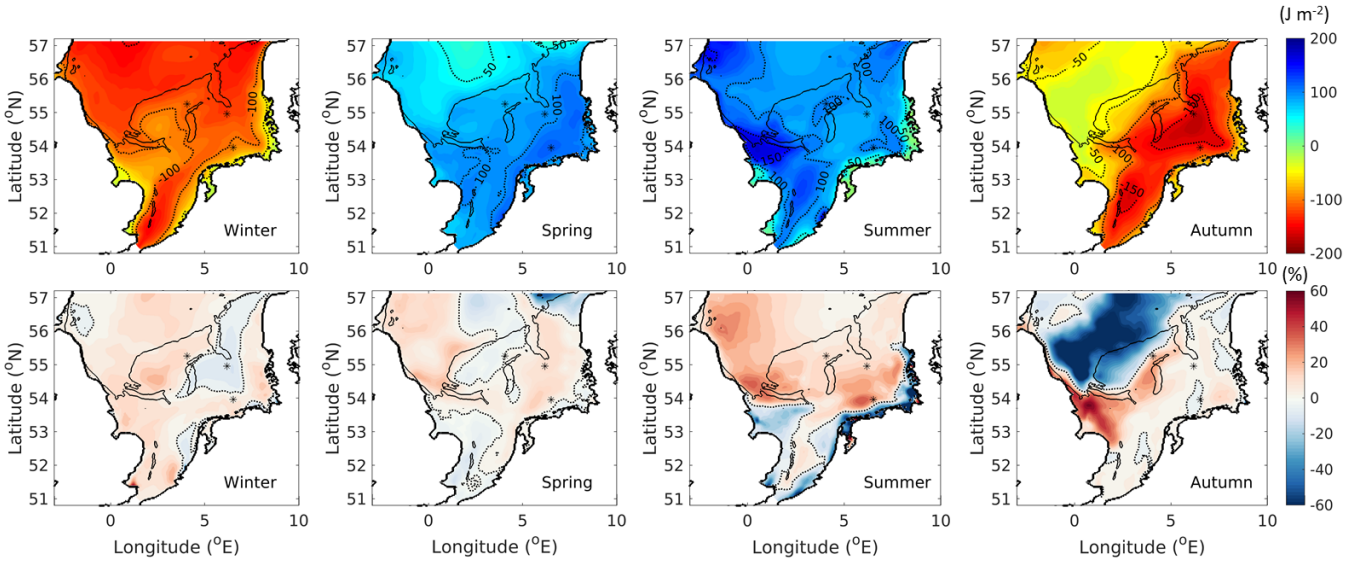

Figure 13. Same as Figure 12, but for the surface heat fluxes. In the upper panels, positive values denote net fluxes from the air to the sea.

the balance between baroclinic forcing and friction, becomes more pronounced with stronger current velocities (larger vertical shear) ~~in warmer climate conditions . Huang et al. (1999) modelled the seasonal thermal stratificationand baroclinic circulation~~ under warmer conditions when the turbulent eddy viscosity is eliminated by the increased stratification. Huang et al. (1999) showed that water transport in the Bohai Sea ~~, where the water depth is shallow (with a maximum of approximately 70 m). They showed an enhancement of water transport by baroclinic circulation from a weakly stratified situation~~ is enhanced from weak stratification in spring to ~~a strongly stratified situation~~ strong stratification in summer. In the North Sea, ~~Lwiza et al. (1991) conducted a study of thermal-induced circulation along tidal mixing fronts in summer. Luyten et al. (1999) further analysed the~~ the relations between the cycle of thermal fronts and baroclinic circulation ~~in the North Sea at different ranges of timescales . They showed the increase/decrease in vertical mixing with the enhancement/reduction of the depth mean temperature in summer through the surface heat flux. Moreover, decreased vertical turbulent mixing reduced~~ were analysed at different timescales (Lwiza et al., 1991; Luyten et al., 1999). Decreased vertical turbulent mixing reduces the magnitude and horizontal shear of ~~the~~ baroclinic currents. This was found to be important feedback from turbulent mixing to the frontal temperature gradients and baroclinic circulation (Luyten et al., 2003)~~. These mechanisms would be pronounced in the case of the extreme events. Schrum et al. (2003) identified unusual stratification~~ and these mechanisms become further pronounced when extreme meteorological events occur. By analysing 40 years of data, Schrum et al. (2003) identified an unusual stratification due to wind and volume transport in the 1990s~~by analysing 40-year data. However, the study was still in a preliminary stage and with a focus on decadal timescale wind impacts on the exchange flow at the open boundaries. .~~ Recently, Chen et al. (2021) investigated the heat budget of the North Sea ~~. They demonstrated that modifying water temperatures by assimilating satellite SST had an impact on the water circulation on an annual timescale and further affected advective heat transport~~ and demonstrated that the

modification of SST affects the advection of water and transport of heat in the North Sea. Comparatively, extreme events, i.e., summer heatwaves, ~~had~~ have more intensive influences on SST~~but within a relatively~~ , albeit on a shorter timescale. ~~Exploring the reaction~~ Certainly, exploring the responses of the regional water circulation to extreme events in the southern North Sea is an interesting topic and deserves further study.

5 Conclusions

This study investigated the influence of extreme ~~climate~~ meteorological events, i.e., European heatwaves, on the occurrence of the summer stratification in the North Sea. With a numerical model that simulated the water temperatures ~~in~~ over multiple years, ~~the~~ this work addressed the question remaining after the study by van Leeuwen et al. (2015): What kind of 'interannual variability' results in the failure ~~of classifying~~ to classify the stratification regimes in one-third of the North Sea~~as one of the defined stratification regimes~~?

Based on the model simulations, a potential energy anomaly was calculated for multiple years in the North Sea model domain. In the southern North Sea, stratification developed from May to August. The intensity of this stratification presented an obvious interannual variation that was related to the occurrence of summer heatwave events. The data from 2018 were analysed as a case study and compared with ~~those of the multiple-year~~ the multiyear mean and the ~~normal year 2015.~~ data during a normal year (i.e., 2015). Regarding the main factors that affect the intensity and duration of the thermal stratification in the southern North Sea, the comparison of temperature data near the water surface and the bottom revealed three aspects. The first was the intense increase in SST ~~in~~ over a short time~~and~~ , the second was a ~~relatively~~ higher water temperature during summer ~~compared to the multiple-year mean. The~~ than the multiyear mean, and the third was the memory of the near-bottom water layer to the low air temperatures during early spring.

By computing the correlation coefficient (R) between the air temperatures and the potential energy anomaly, ~~we identified~~ the region of thermal stratification in the North Sea was identified ($R > 0$). ~~The region covered~~ This region covers the North Sea north of 54°N ~~of the North Sea~~, excluding the permanently stratified Norwegian Trench and the permanently well-mixed coastal seas near the Danish Wadden Sea. ~~Features in stratification were different between the north and south sides at a 50-m depth . Contrary~~ The features of this stratification differed between the northern and southern sides of 54°N at a depth of 50 m. In contrast to the northern part, where the water column was seasonally stratified every year, the southern part was stratified in the years when heatwaves occurred. The dependence of thermal stratification on heatwave events was quantified by the ratio r between the change in the number of water stratification days in ~~2011-2018~~ 2011˘2018 and the change in the number of MHW days during the same period. ~~The~~ A ratio $r = 1$ indicates that the change in the number of thermal stratification days is the same as ~~the change in~~ that of MHW days. Large ratios ($r > 0.8$)were found ~~on the southern side~~ to the south of the 50~~m isobath~~ m isobath (between 6.5°E and the Danish coast~~, which covered~~), covering most of the region left with an unclassified stratification regime ~~of~~ by van Leeuwen et al. (2015).

Water depth appeared to be the factor that controlled the sensitivity of the stratification to ~~the summer heatwave . Apart from~~ summer heatwave events. In addition to proximity to the coast, the ~~stratified period was more~~ stratification period was highly

dependent on the number of days a heatwave event lasted. After analysing the structure of the gradient Richardson number R_i, it was found that heatwave-induced seasonal stratification ~~mainly occurred~~ occurred mainly in the region where the water depth ~~was~~ is between 35 m and 50 m.

This research is the first to link ~~heat wave events with~~ heatwave events to the occurrence and persistence of density stratification in the southern North Sea. In a broader context, this research ~~will~~ is expected to have fundamental significance for further ~~discussion of~~ investigating the secondary effects of ~~heat wave~~ heatwave events, such as in ecosystems, fisheries, and sediment dynamics. With the growing debate regarding the impacts of ~~increasing extreme climate events,~~ increasingly extreme meteorological events, future assessments of these factors will be of ~~more~~ only growing importance in the North Sea~~in the future~~.

Code availability. The model code is available at https://www.nemo-ocean.eu/for NEMO and https://github.com/mywave/WA M for WAM.

Data availability. The outputs of the GCOAST simulations (in NetCDF format) are available upon request to the corresponding author.

Appendix A: Estimates of the ~~oceanic water~~ seawater density

The water density ρ in Eq. 2 is given by

$$\rho(S,T) = \rho_{\mathrm{r}} + \mathrm{A}S + \mathrm{B}S^{\frac{3}{2}} + \mathrm{C}S^2. \tag{A1}$$

In ~~this~~ the above equation, S is the salinity of ~~sea water in ppt (~~seawater in parts per thousand by volume (ppt). The reference density ρ_{r} ~~,~~ and the coefficients A, B and C are also functions of the potential temperature T ~~in (~~^{o}C~~with~~) following the expressions given by Millero and Poisso (1981):

$$\begin{aligned}
\rho_{\mathrm{r}} =& 999.842594 + 6.793952\times10^{-2}T - 9.095290\times10^{-3}T^2 \\
&+ 1.001685\times10^{-4}T^3 - 1.120083\times10^{-6}T^4 \\
&+ 6.536332\times10^{-9}T^5; \\
\mathrm{A} =& 8.24493\times10^{-1} - 4.0899\times10^{-3}T + 7.6438\times10^{-5}T^2 \\
&- 8.2467\times10^{-7}T^3 + 5.3875\times10^{-9}T^4; \\
\mathrm{B} =& -5.72466\times10^{-3} + 1.0227\times10^{-4}T \\
&- 1.6546\times10^{-6}T^2; \\
\mathrm{C} =& 4.8314\times10^{-4}.
\end{aligned}$$

Here, S and T are obtained from the model with a temporal resolution of 6-hours. Moreover, ~~a~~ the 6-hour resolution model output of the sea surface elevation η is taken for computation (see ~~the main text eq~~Eq. 1 and ~~2~~Eq. 2 in the main text).

Author contributions. Wei Chen wrote the article and analysed and interpreted the results. Wei Chen and Joanna Staneva conceived the study. Sebastian Grayek ran the simulations and was responsible for all technical issues of the modelling. Joanna Staneva and Johannes Schulz-Stellenfleth contributed to the writing. Jens Greinert performed the field work and collected observational data.

Competing interests. The authors declare that they have no conflicts of interest.

Acknowledgements. This study is supported by the Digital Earth project (funded by the Helmholtz Association). The authors gratefully acknowledge the German Climate Computing Centre (DKRZ) for providing computing time on the Supercomputer MISTRAL.

References

Alari, V., Staneva, J., Breivik, Ø., Bidlot, J.-R., Mogensen, K., and Janssen, P.: Surface wave effects on water temperature in the Baltic Sea: simulations with the coupled NEMO-WAM model, Ocean Dynamics, 66, 917–930, https://doi.org/10.1007/s10236-016-0963-x, 2016.

Babanin, A. V.: On a wave-induced turbulence and a wave-mixed upper ocean layer, Geophysical Research Letter, 33, 6, https://doi.org/10.1029/2006GL027308, 2006.

Becker, G. A.: Beiträge zur hydrographie und wärmebilanz der Nordsee, Deutsche Hydrografische Zeitschrift, 34, 167–262, https://doi.org/10.1007/BF02225959, 1981.

Bensoussan, N., Romano, J. C., Harmelin, J. G., and Garrabou, J.: High resolution characterization of northwest Mediterranean coastal waters thermal regimes: to better understand responses of benthic communities to climate change, Estuar. Coast. Shelf Sci., 87, 431–441, https://doi.org/10.1016/j.ecss.2010.01.008, 2010.

Bond, N. A., Cronin, M. F., Freeland, H., and Mantua, N.: Causes and impacts of the 2014 warm anomaly in the NE Pacific, Geophys. Res. Lett, 42, 3414–3420, https://doi.org/10.1002/2015GL063306, 2015.

Borges, A., Royer, C., Martin, J. L., Champenois, W., and Gypens, N.: Response of marine methane dissolved concentrations and emissions in the Southern North Sea to the European 2018 heatwave, Continental Shelf Research, 190, 104 004, https://doi.org/https://doi.org/10.1016/j.csr.2019.104004, 2019.

Breivik, Ø., Mogensen, K., Bidlot, J. R., Balmaseda, M. A., and Janssen, P. A. E. M.: Surface wave effects in the NEMO ocean model: Forced and coupled experiments, Journal of Geophysical Research, 120, 2973–2992, https://doi.org/10.1002/2014JC010565, 2015.

Chen, W., Schulz-Stellenfleth, J., Grayek, S., and Staneva, J.: Impacts of the assimilation of satellite sea surface temperature data on volume and heat budget estimates for the North Sea, Journal of Geophysical Research: Oceans, 126, e2020JC017 059, https://doi.org/10.1029/2020JC017059, 2021.

Davies, A. M., Kwong, S. C. M., and Flather, R. A.: On determining the role of wind wave turbulence and grid resolution upon computed storm driven currents, Continental Shelf Research, 20, 1825–1888, https://doi.org/10.1016/S0278-4343(00)00052-2, 2000.

Egbert, G. D. and Erofeeva., S. Y.: Efficient inverse modeling of barotropic ocean tides, Journal of Atmospheric and Oceanic Technology, 19.2, 183–204, 2002.

Elliott, A. and Clarke, T.: Seasonal stratification in the northwest European shelf seas, Continental shelf research, 11, 467–492, https://doi.org/10.1016/0278-4343(91)90054-A, 1991.

Feng, M., McPhaden, M., Xie, S., and Hafner, J.: La Niña forces unprecedented Leeuwin Current warming in 2011, Sci. Rep., 3, 1277, https://doi.org/10.1038/srep01277, 2013.

Fernand, L., Weston, K., Morris, T., Greenwood, N., Brown, J., and Jickells, T.: The contribution of the deep chlorophyll maximum to primary production in a seasonally stratified shelf sea, the North Sea, Biogeochemistry, 113, 153–166, https://doi.org/10.1007/s10533-013-9831-7, 2013.

Fettweis, M., Baeye, M., Van der Zande, D., Van den Eynde, D., and Joon Lee, B.: Seasonality of floc strength in the southern North Sea, Journal of Geophysical Research: Oceans, 119, 1911–1926, https://doi.org/doi.org/10.1002/2013JC009750, 2014.

GEOMAR: RV POSEIDON Fahrtbericht Cruise Report POS526, Helmholtz-Zentrum für Ozenforschung Kiel, 2019.

Günther, H., Hasselmann, S., and Janssen, P. A. E. M.: The WAM model, Cycle 4, Haumburg, 1992.

Herring, S. C., Hoerling, M. P., Kossin, J. P., Peterson, T. C., and Stott, T. C.: INTRODUCTION TO EXPLAINING EXTREME EVENTS OF 2014 FROM A CLIMATE PERSPECTIVE, Bulletin of the American Meteorological Society, 96, S1–S4, 2015.

Hersbach, H., Bell, B., Berrisford, P., Hirahara, S., Horányi, A., Muñoz-Sabater, J., ., and Thépaut, J. N.: The ERA5 global reanalysis, Quarterly Journal of the Royal Meteorological Society, 146, 1999–2049, 2020.

Ho-Hagemann, H. T. M., Gröger, M., Rockel, B., Zahn, M., Geyer, B., and Meier, H.: Effects of air-sea coupling over the North Sea and the Baltic Sea on simulated summer precipitation over Central Europe, Climate Dynamics, 49, 3851–3876, https://doi.org/10.1007/s00382-017-3546-8, 2017.

Hobday, A. J. and Pecl, G. T.: Identification of global marine hotspots: sentinels for change and vanguards for adaptation action, Reviews in fish biology and fisheries, 24, 415–425, https://doi.org/10.1007/s11160-013-9326-6., 2014.

Hobday, A. J., Alexander, L. V., Perkins, S. E., Smale, D. A., Straub, S. C., Oliver, E. C. J., Benthuysen, J. A., Burrows, M. T., Donat, M. G., Feng, M., Holbrook, N. J., Moore, P. J., Scannell, H. A., Sen Gupta, A., and Wernberg, T.: A hierarchical approach to defining marine heatwaves, Progress in Oceanography, 141, 227–238, https://doi.org/10.1016/j.pocean.2015.12.014, 2016.

Hu, Z., Kumar, A., Jha, B., Zhu, J., and Huang, B.: Persistence and predictions of the remarkable warm anomaly in the northeastern Pacific Ocean during 2014–16, J. Clim., 30, 689–702, https://doi.org/10.1175/JCLI-D-16-0348.1, 2017.

Huang, D., Su, J., and Backhaus, J. O.: Modelling the seasonal thermal stratification and baroclinic circulation in the Bohai Sea, Continental Shelf Research, 19, 1485–1505, https://doi.org/10.1016/S0278-4343(99)00026-6, 1999.

Imbery, F., Friedrich, K., Haeseler, S., Koppe, C., Janssen, W., and Bissolli, P.: Vorläufiger Rückblick auf den Sommer 2018 –eine Bilanz extremer Wetterereignisse, Tech. rep., Deutscher Wetterdienst (DWD), 2018.

IPCC: Managing the risks of extreme events and disasters to advance climate change adaptation: special report of the intergovernmental panel on climate change, Cambridge University Press, 2012.

IPCC: AR6 Climate Change 2021: The Physical Science Basis, Cambridge University Press, In Press, 2021.

Klonaris, G., Van Eeden, F., Verbeurgt, J., Troch, P., Constales, D., Poppe, H., and De Wulf, A.: ROMS Based Hydrodynamic Modelling Focusing on the Belgian Part of the Southern North Sea, J. Mar. Sci.Eng., https://doi.org/10.3390/jmse9010058, 2021.

Luyten, P., Jones, J., Proctor, R., Tabor, A., Tett, P., and Wild-Allen, K.: COHERENS—A coupled hydrodynamical–ecological model for regional and shelf seas, user documentation, MUMM, 1999.

Luyten, P. J., Jones, J. E., and Proctor, R.: A numerical study of the long-and short-term temperature variability and thermal circulation in the North Sea, Journal of Physical Oceanography, 33, 37–56, https://doi.org/10.1175/1520-0485(2003)033<0037:ANSOTL>2.0.CO;2, 2003.

Lwiza, K., Bowers, D., and Simpson, J.: Residual and tidal flow at a tidal mixing front in the North Sea, Continental Shelf Research, 11, 1379–1395, https://doi.org/10.1016/0278-4343(91)90041-4, 1991.

Madec, G. and the NEMO team: NEMO ocean engine, Note du Pole de modélisation, Institut Pierre-Simon Laplace (IPSL) No. 27. ISSN-1288-1619, France, 2016.

Manta, G., de Mello, S., Trinchin, R., Badagian, J., and Barreiro, M.: The 2017 record marine heatwave in the southwestern Atlantic shelf, Geophys. Res. Lett., 45, 12 449–12 456, https://doi.org/10.1029/2018GL081070, 2018.

Mathis, M., Elizalde, A., Mikolajewicz, U., and Pohlmann, T.: Progress in Oceanography, 91, 2015.

Merchant, C. J., Embury, O., Bulgin, C. E., Block, T., Corlett, G. K., Fiedler, E., and ... Eastwood, S.: Satellite-based time-series of sea-surface temperature since 1981 for climate applications, Scientific data, 6, 1–18, 2019.

Millero, F. J. and Poisso, A.: International one-atmosphere equation of state of seawater, Ocean Science, 28, 625–629, https://doi.org/10.1016/0198-0149(81)90122-9, 1981.

Nielsen, T. G., Løkkegaard, B., Richardson, R., Pedersen, F. B., and Hansen, L.: Structure of plankton communities in the Dogger Bank area (North Sea) during a stratified situation, Marine Ecology Progress Series, 95, 115–131, 1993.

Oliver, E., Benthuysen, J. A., Bindoff, N. L., Hobday, A. J., and J.Holbrook, N.: The unprecedented 2015/16 Tasman Sea marine heatwave, Nat. Commun., 8, 16 101, https://doi.org/10.1038/ncomms16101, 2017.

Oliver, E. C., Benthuysen, J. A., Darmaraki, S., Donat, M. G., Hobday, A. J., Holbrook, N. J., Schlegel, R. W., and Gupta, A. S.: Marine heatwaves, Annual Review of Marine Science, 13, https://doi.org/doi.org/10.1146/annurev-marine-032720-095144, 2020.

Otto, L., Zimmerman, J. T. F., Furnes, G. K., Mork, M., Sætre, R., and Becker, G.: Review of the physical oceanography of the North Sea., Netherlands Journal of Sea Research, 26, 161–238, https://doi.org/10.1016/0077-7579(90)90091-T, 1990.

O'Dea, E. J., Arnold, A. K., Edwards, K. P., Furner, R., Hyder, P., Martin, M. J., Siddorn, J. R., Storkey, D., While, J., Holt, J. T., and Liu, H.: An operational ocean forecast system incorporating NEMO and SST data assimilation for the tidally driven European North-West shelf, Journal of Operational Oceanography, 5, 3–17, https://doi.org/10.1080/1755876X.2012.11020128, 2012.

Pearce, A. F., Lenanton, R., Jackson, G., Moore, J., Feng, M., and Gaughan, D.: The "marine heat wave" off Western Australia during the summer of 2010/11, vol. 222, Fisheries Research Report, Western Australian Fisheries and Marine Research Laboratories, 2011.

Perkins, S. E. and Alexander, L. V.: On the measurement of heat waves, Journal of Climate, 26, 4500–4517, https://doi.org/10.1175/JCLI-D-12-00383.1, 2013.

Perkins-Kirkpatrick, S., King, A., Cougnon, E., Holbrook, N., Grose, M., ..., and Pourasghar, F.: The role of natural variability and anthropogenic climate change in the 2017/18 Tasman Sea marine heatwave, Bull. Am. Meteorol. Soc, 100, S105–10, https://doi.org/10.1175/BAMS-D-18-0116.1, 2019.

Pingree, R. and Griffiths, D.: Tidal fronts on the shelf seas around the British Isles, Journal of Geophysical Research: Oceans, 83, 4615–4622, https://doi.org/10.1029/JC083iC09p04615, 1978.

Pohlmann, T.: Calculating the development of the thermal vertical stratification in the North Sea with a three-dimensional baroclinic circulation model, Continental Shelf Research, 16, 163–194, https://doi.org/10.1016/0278-4343(95)00018-V, 1996.

Rouault, M., Illig, S., Bartholomae, C., Reason, C., and Bentamy, A.: Propagation and origin of warm anomalies in the Angola Benguela upwelling system in 2001, J. Mar. Syst., 68, 473–488, https://doi.org/10.1016/j.jmarsys.2006.11.010, 2007.

Sas, H., Didderen, K., van der Have, T., Kamermans, P., van den Wijngaard, K., and Reuchlin-Hugenholtz, E.: Recommendations for flat oyster restoration in the North Sea, Tech. rep., Sas Consultancy, 2019.

Schrum, C., Siegismund, F., and St John, M.: Decadal variations in the stratification and circulation patterns of the North Sea. Are the 1990s unusual, in: ICES J Mar Sci, Symp Ser, vol. 219, pp. 121–131, 2003.

Sharples, J., Ross, O. N., Scott, B. E., Greenstreet, S. P. R., and Fraser, H.: Inter-annual variability in the timing of stratification and the spring bloom in the North-western North Sea, Continental Shelf Research, 26, 733–751, 2006.

Simpson, J. H.: The shelf-sea fronts: implications of their existence and behaviour, Philosophical Transactions of the Royal Society of London. Series A, Mathematical and Physical Sciences, 302, 531–546, https://doi.org/10.1098/rsta.1981.0181, 1981.

Simpson, J. H., Charnock, H., Dyer, K. R., Huthnance, J. M., Liss, P. S., and Tett, P. B.: Understanding the North Sea System, Springer, Netherlands, 1994.

Smale, D. A., Wernberg, T., Oliver, E. C. J., Thomsen, M., Harvey, B. P., Straub, S. C., Burrows, M. T., Alexander, L. V., Benthuysen, J. A., and Donat, M. G. . e. a.: Nature: Climate Change, 9, 306–312, https://doi.org/10.1038/s41558-019-0412-1, 2019.

Staneva, J., Alari, V., Breivik, O., Bidlot, J. R., and Mogensen, K.: Effects of wave-induced forcing on a circulation model of the North Sea., Ocean Dynamics, 67, 81–191, https://doi.org/10.1007/s10236-016-1009-0, 2017.

Staneva, J., Ricker, M., Carrasco-Alvarez, R., Breivik, Ø., and Schrum, C.: Effects of Wave-Induced Processes in a Coupled Wave–Ocean Model on Particle Transport Simulations, Water, 13, 473–488, https://doi.org/10.3390/w13040415, 2021.

Stathopoulos, C., Galanis, G., and Kallos, G.: A coupled modeling study of mechanical and thermodynamical air-ocean interface processes under sea storm conditions, Dynamics of Atmospheres and Oceans, 91, 101 140, https://doi.org/10.1016/j.dynatmoce.2020.101140, 2020.

Stips, A., Bolding, K., Pohlmann, T., and Burchard, H.: Simulating the temporal and spatial dynamics of the North Sea using the new model GETM (general estuarine transport model), Ocean Dynamics, 54, 266–283, https://doi.org/10.1007/s10236-003-0077-0, 2004.

Tan, H. and Cai, R.: What caused the record-breaking warming in East China Seas during August 2016?, Atmos. Sci. Lett., 19, 853, https://doi.org//10.1002/asl.853, 2018.

The Wamdi Group: The WAM Model—A Third Generation Ocean Wave Prediction Model, Journal of Physical Oceanography, 18, 1775–1810, https://doi.org/10.1175/1520-0485(1988)018<1775:TWMTGO>2.0.CO;2, 1988.

Umlauf, L. and Burchard, H.: A generic lengthscale equation for geophysical turbulence models, Journal of Marine Research, 61, 235–265, https://doi.org/10.1357/002224003322005087, 2003.

van Haren, H.: Properties of vertical current shear across stratification in the North Sea, Journal of Marine Research, 58, 465–491, https://doi.org/10.1357/002224000321511115, 2000.

van Leeuwen, S., Tett, P., Mills, D., and van der Molen, J.: Stratified and nonstratified areas in the North Sea: Long-term variability and biological and policy implications, Journal of Geophysical Research: Oceans, 120, 4670–4686, https://doi.org/10.1002/2014JC010485, 2015.

Wakelin, S., Townhill, B., Engelhard, G., Holt, J., and Renshaw, R.: in: Copernicus Marine Service Ocean State Report, Issue 5, edited by von Schuckmann, K., Le Traon, P.-Y., Smith, N., Pascual, A., Djavidnia, S., and Gattuso, J.-P. . e. a., vol. 14, p. 185, https://doi.org/10.1080/1755876X.2021.1946240, 2021.

Wernberg, T., Smale, D. A., Tuya, F., Thomsen, M. S., Langlois, T. J., De Bettignies, T., Bennett, S., and Rousseaux, C. S.: An extreme climatic event alters marine ecosystem structure in a global biodiversity hotspot, Nature Climate Change, 3, 78–82, https://doi.org/10.1038/NCLIMATE1627, 2013.

Wernberg, T., Bennett, S., Babcock, R. C., De Bettignies, T., Cure, K., Depczynski, M., Dufois, F., Fromont, J., Fulton, C. J., Hovey, R. K., et al.: Climate-driven regime shift of a temperate marine ecosystem, Science, 353, 169–172, https://doi.org/10.1126/science.aad8745, 2016.

Wu, L., Staneva, J., Breivik, O., Rutgersson, A. adn George Nurser, A. J., Clementi, E., and Madec, G.: Wave effects on coastal upwelling and water level, Ocean Modelling, 140, 101 405, https://doi.org/10.1016/j.ocemod.2019.101405, 2019.

https://link.springer.com/article/10.1007/s00704-020-03166-8